Extended Abstracts of the 2007 International Conference on Solid State Devices and Materials, Tsukuba, 2007, pp. 372-373

P-1-25L

Oxygen-Vacancy-Induced V_t shift in La-containing Devices

B.J. O'Sullivan, R. Mitsuhashi[1], G. Pourtois, V.S. Chang[2], C. Adelmann, T. Schram, L.-Å. Ragnarsson, N. Van der Heyden[5], H.-J. Cho[3], Y. Harada[4], A. Veloso, R. O'Connor, L. Pantisano, H.Y. Yu, G. Groeseneken[5], P. Absil, S. Biesemans, A. Ikeda[1], M. Niwa[4]

IMEC, Kapeldreef 75, B-3001 Leuven, Belgium, assignee at IMEC from[1] Matsushita Ltd. [2] TSMC, [3] Samsung, [4]Matsushita Electric Industrial Co. Ltd., Japan [5] IMEC and also at KU, Leuven. E-mail: osullivb@imec.be

For the first time, we report an anomalous negative PBTI and positive NBTI shift for La_2O_3 capped HfSiON dielectrics. These result from electrically active oxygen vacancies in the high-κ dielectric, inherent due to the differences in electronic configuration between Lanthanum and Hafnium. Controlled activation of these defects, through electrode workfunction tuning and cap layer thickness engineering can result in a 350 mV V_t reduction, with no reliability degradation.

Introduction

In the bid to engineer workfunction (WF) values for (sub-) 32nm CMOS, rare earth oxide capping of high-κ dielectrics have recently emerged as a possible, attractive route. La incorporation has been shown to reduce nMOS V_t values by up to 500 mV [1,2]. The origin of the V_t shift is still uncertain, with the possible sources ranging from oxygen vacancies, La-induced electronegativity tuning [3], structural distortions [4], or dipole formation at the high-κ/SiO_2 interface [5]. However, these models do not fully explore the effect of the electrode or its WF on the V_t shift, and the bias temperature instability characteristics have not been investigated in detail thus far. In this work, we provide a comprehensive understanding of these phenomena, which are of paramount importance in evaluating the feasibility of using this capping-layer technology in future generation CMOS nodes.

Experimental

Devices were fabricated with 1-nm La_2O_3 capping layers deposited by ALD on MOCVD or ALD HfSiON nMOS devices. PVD TaC_x, PVD TaC_xN_y and CVD TaC_xN_y were considered as gate electrodes. All samples experienced a spike anneal at 1030°C. EOT values extracted range from 10-16 Å.

Results

The effect of La_2O_3 capping on CV and $V_{t\,lin}$ characteristics are highlighted in figure 1, where V_{fb} and V_t are reduced, with V_t reduced by ~500 mV, ~200 mV and ~300 mV for PVD TaC_x, PVD TaC_xN_y and CVD TaC_xN_y, respectively (in inset). BTI analysis was performed at 373K (unless specified), with a fast (0.5s) measurement step to ensure minimum defect recovery during the sense process. The PBTI characteristics measured on the reference and capped TaC_x are displayed in figure 2 (inset), where it is clear that the cap has the effect of inducing a *negative* V_t shift, with increasing E_{ox}. This is not the case for PVD TaC_xN_y (figure 3), where a standard positive shift is observed. The difference in nitrogen content in the electrode is not believed to affect the dielectrics, as all received the same nitridation step prior to cap deposition. The effect of the nitridation is a modification of the WF of the electrode itself. If the BTI polarity is reversed, and the results are plotted together with the PBTI data (figures 2 and 3 for PVD TaC_x and PVD TaC_xN_y), it is clear that both the N and PBTI results from the TaC_x film are in the opposite direction than expected. That the N and PBTI degradation for PVD TaC_x (Figure 2) overlap with increasing stress condition indicates the defects responsible are pre-existing rather than stress-induced, which is not observed for the PVD TaC_xN_y film (Figure 3), indicating a different phenomenon is responsible for the degradation. A positive V_t shift during NBTI has previously been attributed to negative charge in the high-κ dielectric, but in this case the PBTI was positive [6]. Nonetheless, the electrode-dependent effect signals a non-equilibrium condition in the stack, where the La-containing stacks are less thermodynamically stable than the reference counterparts.

The La_2O_3 intermixes with HfSiON [2]. This is also evident from XRR data in figure 4, and from TEM in the inset [2]. Models to the XRR data of the as grown sample are consistent with chemically abrupt interfaces. After annealing at 1000°C, the almost complete disappearance of the interference fringes indicates strong intermixing between La_2O_3 and $HfSiO_x$.

Discussion: Electrically active oxygen vacancy model

Oxygen vacancies are inevitable in these stacks, given the difference in co-ordination with oxygen for La (1.5) and Hf (2), as shown schematically in Figure 5. The observations in figures 2 and 3 could be explained by results from first-principle (DFT-GGA) simulations, which show the presence of the resultant oxygen vacancies in the La_2O_3 bandgap, at energy levels in the region of the WF of the electrodes used. These vacancies result in the WF/V_t reduction observed in all samples with La_2O_3 cap [7, 8]. The further negative shift observed in TaC_x could be explained by activation of another defect band of oxygen vacancies in the high-κ bandgap, at an energy level higher than accessible for the TaC_xN_y-gated stacks. A schematic band diagram is presented in figure 6 to explain the measured P and NBTI phenomena.

The results from N and PBTI for PVD TaC_x, PVD TaC_xN_y and CVD TaC_xN_y are presented in figure 7. It is evident that the TaC_xN_y behaviour is independent of deposition method. BTI in capped TaC_x stacks are strongly temperature dependent (E_a ~0.18 eV, PBTI, ~0.15 eV NBTI), from figure 8. That the response is quite symmetric suggests that the oxygen vacancies are amphoteric, and are accessed by both injection polarities, i.e. are distributed throughout the high-κ (figure 6).

Model consequences

The effect of La_2O_3 thickness on V_t reduction is shown in the inset of Figure 9, where the V_t reduction reaches up to 500 mV at 1 nm of La_2O_3. EOT increase was less than 0.5Å. However, the PBTI measured (at constant V_g-V_t) reduces with increasing La_2O_3 thickness above 5 Å, in Figure 9. An optimum is reached at ΔV_t ~350mV, at which point the La content is sufficiently low to control the oxygen vacancy density, thereby preventing the negative PBTI and positive NBTI phenomena. Negligible PBTI with ~250 mV V_t reduction agrees with a recent report [5]. This result is consistent for cap layers with various electrodes from both N and PBTI analysis, shown in Figure 10. This suggests a contribution of the electrode WF on the electrical activity of oxygen vacancies, whose inherent density is determined by the La content in the film, and the combination of these factors result in the V_t reduction.

Conclusions

Optimised La_2O_3-capped HfSiON layers can reduce nMOS V_t by 350 mV, combined with TaC_x gate, without degrading device reliability. Further increase in lanthanum content results in anomalous bias temperature instabilities. This occurs due to electrical activity of inherent oxygen vacancies in the dielectric, whose density is determined by the lanthanum content. Magnitude of V_t tuning was shown to be determined by vacancy density and level of activation, set by the cap thickness and metal workfunction, respectively.

References

[1] Kirsch et.al., IEDM 2006, [2] Ragnarsson et.al., EDL, **28**, 2007, p486, [3] Narayanan et.al., VLSI 2006, [4] Wang et.al., EDL, **27**, 2006, p31, [5] Sivasubramani et.al., VLSI 2007 [6] Jung et.al. IRPS, 2005, [7] Van Der Heyden et.al., to be presented at ECS 2007 [8] Cartier et al, VLSI, 2005

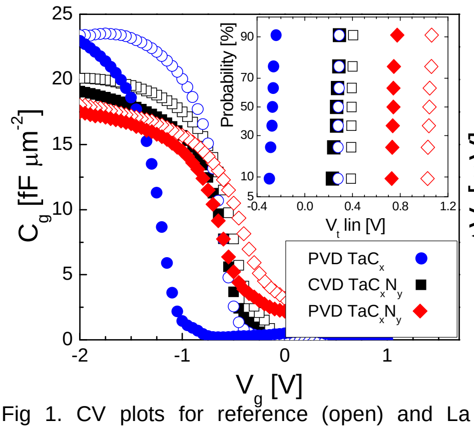

Fig 1. CV plots for reference (open) and La capped (solid) films with PVD TaC$_x$, PVD TaC$_x$N$_y$ and CVD TaC$_x$N$_y$ electrodes. V_t distributions for capped and reference samples shown in inset

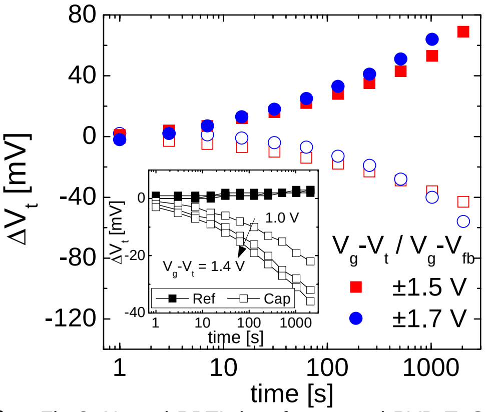

Fig 2. N- and PBTI data for capped PVD TaC$_x$. Open symbols for PBTI, solid for NBTI. Inset shows PBTI compared to uncapped reference

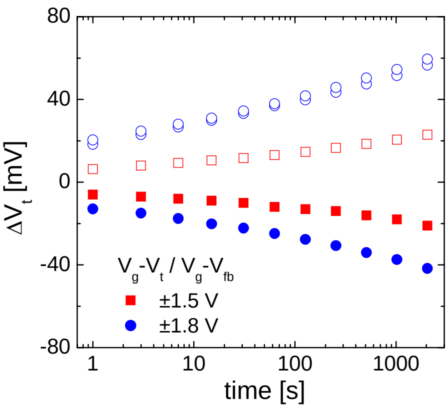

Fig 3. N and PBTI data for La-capped PVD TaC$_x$N$_y$. Open symbols for PBTI, solid for NBTI

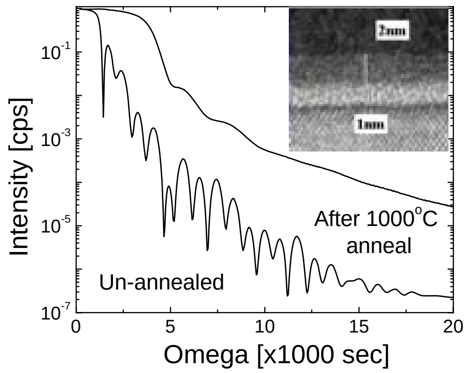

Fig 4. XRR spectrum before and after 1000ºC anneal. The absence of fringing indicates intermixing due to the anneal, also seen in the TEM [2], in the inset

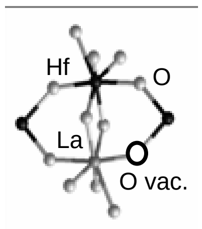

Fig 5. Schematic diagram of bonding co-ordination difference between La_2O_3 and HfSiON, which inevitably results in oxygen vacancies in the dielectric stacks considered

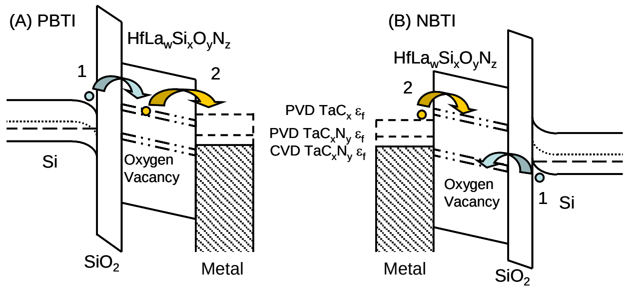

Fig 6. Band diagram to explain phenomena observed during (A) PBTI and (B) NBTI. Two defect bands are present in high-κ, which (1) trap electrons in the upper defect level during PBTI, and holes in the lower level during NBTI in the case of TaC$_x$N$_y$, or (2) de-trap electrons during PBTI and trap electrons during NBTI of TaC$_x$ gated stacks.

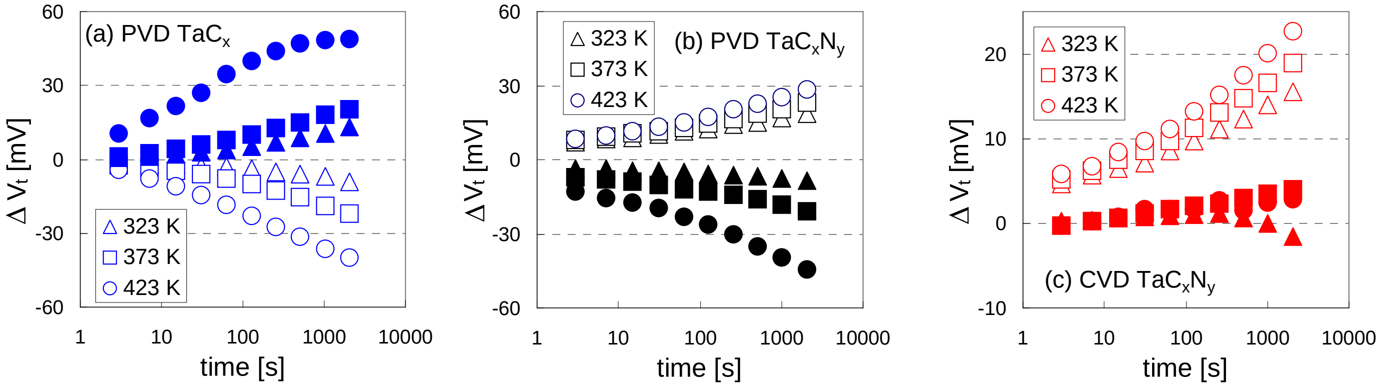

Fig 7. Summary of PBTI (open) and NBTI (filled) findings at different temperatures for (a) PVD TaC$_x$, (b) PVD TaC$_x$N$_y$ and (c) CVD TaC$_x$N$_y$. Measured at similar V_g-V_t or $|V_g$-$V_{fb}|$. Opposite V_t shifts observed for TaC$_x$ electrode, compared to TaC$_x$N$_y$

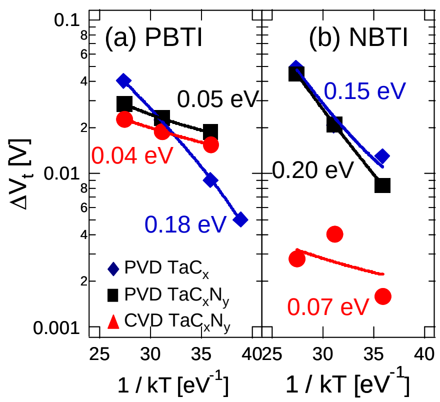

Fig 8. Summary of (a) PBTI and (b) NBTI results. Thermally activated PBTI observed for PVD TaC$_x$. NBTI thermally activated for PVD TaC$_x$, and PVD TaC$_x$N$_y$ (but ΔV_t in opposite direction)

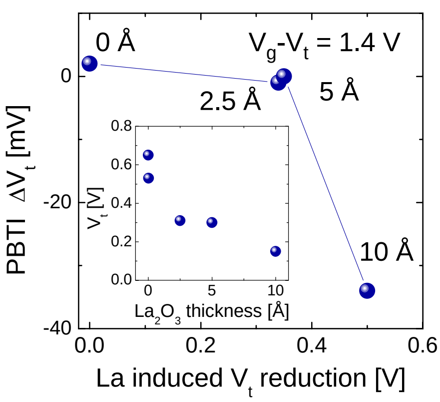

Fig 9. PBTI measured after 2000s stress for PVD TaC$_x$-gated samples, versus the V_t reduction (with respect to uncapped reference, inset) for a series of cap thicknesses. EOT between 10.8 and 11.3 Å

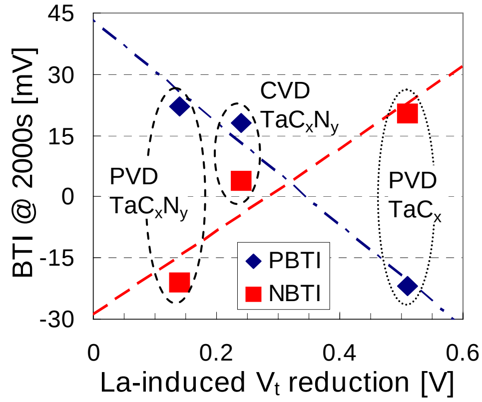

Fig 10. N and PBTI measured after 2000s stress for several metal gated samples, versus the V_t reduction (wrt uncapped reference).